*ENGINEERING TRANSACTIONS* • *Engng. Trans.* • 40, 2, 213–228, 1992
Polish Academy of Sciences • Institute of Fundamental Technological Research

# UNIVERSAL ALGORITHM FOR GENERATION OF MATRICES USED IN DYNAMICS OF CIRCULAR TIMOSHENKO SEGMENTS

B. OLSZOWSKI (KRAKÓW)

The paper deals with a numerical generation of the basic solutions for a set of ordinary differential equations governing the plane vibration of a circular Timoshenko segment and having the normal Cauchy's form. The generation algorithm arose as further development of author's method described in [1] and enables to analyse the stationary harmonic motion of the segment for any boundary conditions and arbitrary values of physical parameters. Numerical calculations are restricted to the analysis of simply supported segments only. For testing purposes, however, this analysis is performed for three types of models: Rayleigh-Timoshenko (RT) and Bernoulli-Euler models with extensible (BEe) or inextensible (BEi) axis. The results of eigenfrequency calculations are plotted and tabulated.

## NOTATIONS

| | | | |
|---|---|---|---|
| $U$ | = | $\bar{U}/L$ | radial displacement, |
| $W$ | = | $\bar{W}/L$ | tangential displacement, |
| $\Phi$ | = | $\bar{\Phi}$ | angular displacement, |
| $Q$ | = | $L^2\bar{Q}/(EI)$ | shear force, |
| $N$ | = | $L^2\bar{N}/(EI)$ | axial force, |
| $M$ | = | $L\bar{M}/(EI)$ | bending moment, |
| $p^2$ | = | $\mu\bar{A}L^4\omega^2/(EI)$ | circular frequency, |
| $f$ | = | $4p/\pi^2$ | comparative frequency, |
| $r$ | = | $J/(\bar{A}L^2)$ | moment of rotary inertia, |
| $\nu_1$ | = | $1,\ \nu_2 = EI/(L^2EA),\ \nu_3 = EI/(L^2kGA)$, | |
| $\xi$ | | | coordinate measured along the axis, |
| $2\alpha$ | | | subtending angle of the arc. |

## 1. INTRODUCTION

Applications of the displacement method in dynamical analysis of complex bar structures performing stationary and harmonic vibration are known from the early 1940's [2]. Advantages of this method, leading to accurate results without any approximations (within the framework of the accepted theoretical model), was the reason that it has been applied and developed successfully by many authors. Some Swedish papers dealing with this subject are of particular interest.

In 1972, B. ÅKESSON, H. TÄGNFORS and O. JOHANNESSON published a detailed description [3] of an exact displacement method and its applications in dynamics of beams and frames analysed within the framework of the Bernoulli - Euler theory. Two years later B. ÅKESSON and H. TÄGNFORS described in [4] a computer program PFVIBAT for dynamical analysis of plane frames, making use of the Wittrick - Williams general algorithm [5]. In 1978 and 1980 new versions of programs PFVIBATII and SVIBATII were worked out. Further application of the method for Rayleigh - Timoshenko bars in space taking into account vibration damping was discussed by R. LUNDEN and B. ÅKESSON in [6]. P.O. FRIBERG [7, 8] described generalizations for uniform beam elements of an open thin-walled cross-section derived from Vlasov's or Euler - Bernoulli - Saint Venant's theories. Papers [3 - 8] contain exhaustive specification and discussion of the corresponding literature.

Applications of the Rayleigh - Timoshenko theory in dynamics of circular rings were described and recapitulated by M.S. ISSA, T.M. WANG and B.T. HSIAO in [9] and T.M. WANG and M.S. ISSA in [10].

The aim of the present paper is the discussion of further applications of the algorithm described in [1] and used there in dynamical analysis of circular Timoshenko rings. It appears that this algorithm may be rearranged in a simple way to become a universal generator of the basic solutions for a set of the ordinary differential equations having the normal Cauchy's form and governing the natural vibration of the Timoshenko segment. Universality of the generator consists in the fact that it may be used in three different ways: 1) for solving eigenproblems of single segments with any boundary conditions, 2) for generating dynamic stiffness and 3) dynamic flexibility matrices of the segments. Thus a basic tool for numerical computation was created, enabling us to improve and widen the range of application of the Wittrick - Williams general algorithm [5] in the dynamical analysis of the complex bar structures in both the displacement and the force versions.

Because of the variety of the base-generator application problems, framework of the present paper has been restricted to the analysis of single segment eigenproblems only, but with arbitrarily chosen boundary conditions. Numerical computations were realized in more narrow range, namely for simply supported segments only. For testing purposes these computations were performed for three types of models: 1) Rayleigh-Timoshenko (RT) and Bernoulli-Euler models with extensible (BEe) or inextensible axis (BEi). The results of computations were plotted and tabulated as functions of the subtending angle $2\alpha$ of the arc.

## 2. General algorithm

Construction of the algorithm is based on the normal Cauchy set of ordinary differential equations [1]

$$\mathbf{X}'(\beta) = \mathbf{L}(\omega)\mathbf{X}(\beta) \tag{2.1}$$

governing the stationary harmonic vibration of a plane Timoshenko segment with circular frequency $\omega$. The unknown vector function

$$\mathbf{X}(\beta) = [U(\beta), W(\beta), \Phi(\beta), Q(\beta), N(\beta), M(\beta)]^T \tag{2.2}$$

represents the state vector of the cross-section with angle coordinate $\beta$.

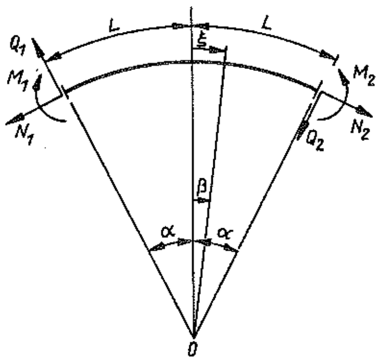


Fig. 1.

Let us consider a segment of circular Timoshenko ring shown in Fig.1, with subtending angle $2\alpha$. Length of the segment is $2L$. For convenience we introduce a new normalized dimensionless coordinate $\xi = \beta/\alpha = s/L$, taking its values from interval $-1.0 \leq \xi \leq +1.0$ and we change, in comparison with [1], the sign convention for $Q$ and $N$ forces. Consequently, we have to introduce into Eq.(2.1) the relationship $\beta = \alpha\xi$ and to transform adequately the matrix L. Using the sign convention as shown in Fig.1 and denoting by $\mathbf{L}_0$, $\mathbf{X}_0$ the matrices occurring in [1], we have

$$\mathbf{X} = \mathbf{T}\mathbf{X}_0, \quad \mathbf{T} = \mathrm{diag}(1,1,1,-1,-1,1),$$

$$\mathbf{L} = \mathbf{T}\mathbf{L}_0\mathbf{T} = \begin{bmatrix} \mathbf{L}_{11} & \mathbf{L}_{12} \\ \mathbf{L}_{21} & \mathbf{L}_{22} \end{bmatrix}, \quad \mathbf{L}_{11} = \begin{bmatrix} 0 & -\alpha & 1 \\ \alpha & 0 & 0 \\ 0 & 0 & 0 \end{bmatrix}, \quad \mathbf{L}_{22} = \begin{bmatrix} 0 & -\alpha & 0 \\ \alpha & 0 & 0 \\ -1 & 0 & 0 \end{bmatrix}.$$

$$\mathbf{L}_{12} = -\mathrm{diag}(\nu_3, \nu_2, \nu_1), \quad \mathbf{L}_{21} = p^2\mathbf{M} = p^2\mathrm{diag}(1,1,r).$$

We assume that solutions of Eq.(2.1) have the general form

$$\mathbf{X}(\xi) = \mathbf{a}e^{\lambda\xi}. \tag{2.3}$$

Substituting (2.3) into (2.1) we get the following algebraic matrix equation for the unknown vector $\mathbf{a}$

$$[\mathbf{L}(\omega) - \lambda\mathbf{I}]\mathbf{a} = \mathbf{0} \tag{2.4}$$

having nontrivial solutions for some discrete values of $\lambda$ only. These values are related by formula $\lambda = \pm\sqrt{\chi}$ to the roots of equation

$$\det[\mathbf{L}(\omega) - \lambda\mathbf{I}] = \chi^3 + K_2\chi^2 + K_1\chi + K_0 = 0. \tag{2.5}$$

The coefficients $K_i$ are real and depend on physical parameters of the model as follows:

$$\begin{aligned} K_2 &= 2\alpha^2 + (r\nu_1 + \nu_2 + \nu_3)p^2, \\ K_1 &= \alpha^4 + [\alpha(\alpha-2)(\nu_2+\nu_3) + \nu_1(2\alpha^2 r - 1)]p^2 \\ &\qquad + [\nu_2\nu_3 + r\nu_1(\nu_2+\nu_3)]p^4, \\ K_0 &= \nu_1 p^2\{\alpha^2(r\alpha^2+1) - [\nu_2 + r\alpha(2-\alpha)(\nu_2+\nu_3)]p^2 + r\nu_2\nu_3p^4\}. \end{aligned} \tag{2.6}$$

Solution of the algebraic eigenproblem (2.4) is composed of six eigenpairs $(\lambda_k, \mathbf{a}_k)$ $k = 1,2,\ldots,6$ defining six linearly independent basic solutions

$$\mathbf{X}_k(\xi) = \mathbf{a}_k e^{\lambda_k\xi}, \qquad k = 1,2,\ldots,6. \tag{2.7}$$

Introduction of matrices

$$\mathbf{\Lambda} = \mathrm{diag}(\lambda_1, \lambda_2, \ldots, \lambda_6), \qquad \mathbf{A} = (\mathbf{a}_1, \mathbf{a}_2, \ldots, \mathbf{a}_6), \tag{2.8}$$

enables us to represent the solution basis as

$$\overset{*}{\mathbf{X}}(\xi) = \mathbf{A}e^{\mathbf{\Lambda}\xi} = (\mathbf{a}_1e^{\lambda_1\xi}, \mathbf{a}_2e^{\lambda_2\xi}, \ldots, \mathbf{a}_6e^{\lambda_6\xi}). \tag{2.9}$$

This basis may be decomposed into the displacement and force components, and in this case we have

$$\overset{*}{\mathbf{X}}(\xi) = \begin{bmatrix} \mathbf{R}(\xi) \\ \mathbf{S}(\xi) \end{bmatrix} = \begin{bmatrix} \mathbf{A}' \\ \mathbf{A}'' \end{bmatrix} e^{\Lambda\xi}, \qquad \mathbf{A} = \begin{bmatrix} \mathbf{A}' \\ \mathbf{A}'' \end{bmatrix}. \tag{2.10}$$

Assuming that $\xi = -1.0$ and $\xi = +1.0$, respectively, we obtain two different vector bases related to both boundary cross-sections of the bar

$$\begin{aligned} \overset{*}{\mathbf{X}}(-1.0) &= \begin{bmatrix} \mathbf{R}(-1.0) \\ \mathbf{S}(-1.0) \end{bmatrix} = \begin{bmatrix} \mathbf{A}' \\ \mathbf{A}'' \end{bmatrix} e^{-\Lambda}, \\ \overset{*}{\mathbf{X}}(+1.0) &= \begin{bmatrix} \mathbf{R}(+1.0) \\ \mathbf{S}(+1.0) \end{bmatrix} = \begin{bmatrix} \mathbf{A}' \\ \mathbf{A}'' \end{bmatrix} e^{\Lambda}. \end{aligned} \tag{2.11}$$

Generation of these two bases is the main operation of the algorithm because it provides all information necessary for computation of the eigenspectra and of both the dynamical stiffness and flexibility matrices of the vibrating segment.

### *2.1. Solution of eigenproblems*

Let us use the following definition

$$\mathbf{e}_i = (0, 0, \ldots, 0, 1_i, 0, \ldots, 0)$$

and the binary selection matrix $\mathbf{d}(i,j,k)$ of dimensions $3 \times 6$ defined as

$$\mathbf{d}^T(i,j,k) = (\mathbf{e}_i^T, \mathbf{e}_j^T, \mathbf{e}_k^T), \quad 1 \le i,j,k \le 6.$$

In order to fulfil any segment's boundary conditions we have to solve a set of homogeneous algebraic equations

$$\begin{bmatrix} \mathbf{d}(i,j,k)\overset{*}{\mathbf{X}}(-1.0) \\ \mathbf{d}(l,m,n)\overset{*}{\mathbf{X}}(+1.0) \end{bmatrix} \mathbf{c} = \mathbf{0}. \tag{2.12}$$

This equation is generated by means of two selection matrices corresponding to the given boundary conditions. Equation (2.12) has non-trivial vector solutions $\mathbf{c}_i$ for a discrete set of parameter values $p = (p_1, p_2, \ldots)$ representing the eigenfrequency spectrum of the segment under consideration. The corresponding set of vector solutions $\mathbf{c} = (\mathbf{c}_1, \mathbf{c}_2, \ldots)$ represents, in turn, the generalized eigenmodes of the segment according to the formula

$$\mathbf{X}_l(\xi) = \overset{*}{\mathbf{X}}(\xi)\mathbf{c}_l, \qquad l = 1, 2, 3, \ldots. \tag{2.13}$$

*2.2. Generation of dynamic stiffness matrix*

Let us rearrange bases (2.11) assuming $\mathbf{d}_1 = \mathbf{d}(1,2,3)$, $\mathbf{d}_2 = \mathbf{d}(4,5,6)$ in order to obtain two new bases

$$\overset{*}{\mathbf{R}} = \begin{bmatrix} \mathbf{d}_1 \overset{*}{\mathbf{X}}(-1.0) \\ \mathbf{d}_1 \overset{*}{\mathbf{X}}(+1.0) \end{bmatrix} = \begin{bmatrix} \mathbf{R}(-1.0) \\ \mathbf{R}(+1.0) \end{bmatrix},$$

$$\overset{*}{\mathbf{S}} = \begin{bmatrix} \mathbf{d}_2 \overset{*}{\mathbf{X}}(-1.0) \\ -\mathbf{d}_2 \overset{*}{\mathbf{X}}(+1.0) \end{bmatrix} = \begin{bmatrix} \mathbf{S}(-1.0) \\ -\mathbf{S}(+1.0) \end{bmatrix}.$$

Minus sign in the last formula takes into account the sign convention used in the displacement method.

Any boundary displacement vector $\mathbf{R}_k$ may be represented as

$$\mathbf{R}_k = \overset{*}{\mathbf{R}}\, \mathbf{c}_k$$

using its coordinates in relation to basis $\overset{*}{\mathbf{R}}$ setting up a vector

$$\mathbf{c}_k = \left(\overset{*}{\mathbf{R}}\right)^{-1} \mathbf{R}_k .$$

Let us consider now a set of vectors $\{\mathbf{R}_k\}$ $k = 1,2,\ldots,6$ equivalent to the unit matrix $\mathbf{I}$. In such a case the corresponding set of vectors $\{\mathbf{c}_k\}$ creates evidently a matrix $(\overset{*}{\mathbf{R}})^{-1}$ denoted below as $\mathbf{C}$. We have now the formulae

$$\overset{*}{\mathbf{R}}\,\mathbf{C} = \mathbf{I}, \qquad \overset{*}{\mathbf{S}}\,\mathbf{C} = \mathbf{K}$$

enabling the following interpretations. Matrix $\mathbf{K}$ is a base matrix composed of the boundary forces corresponding to the unit base matrix composed of boundary displacements. Therefore, matrix $\mathbf{K}$ may be treated as the dynamical stiffness matrix of the segment corresponding to a fixed value of the circular frequency $\omega$.

*2.3. Generation of dynamic flexibility matrix*

A reasoning anologous to the foregoing one leads to the following representation for any boundary force vector

$$\mathbf{S}_k = \overset{*}{\mathbf{S}}\, \mathbf{c}_k .$$

Therefore we obtain $\mathbf{c}_k = \left(\overset{*}{\mathbf{S}}\right)^{-1} \mathbf{S}_k$, $k = 1, 2, \ldots, 6$. If we consider now a set of vectors $\{\mathbf{S}_k\}$ equivalent to the unit matrix $\mathbf{I}$, we shall obtain the corresponding set of vectors $\{\mathbf{c}_k\}$ forming the matrix $\left(\overset{*}{\mathbf{S}}\right)^{-1}$. Denoting this matrix by $\mathbf{C}$ we obtain the formulae

$$\overset{*}{\mathbf{S}}\,\mathbf{C} = \mathbf{I}, \qquad \overset{*}{\mathbf{R}}\,\mathbf{C} = \mathbf{D}\,,$$

and we may introduce the following interpretations. Matrix $\mathbf{D}$ is a base matrix composed of the boundary displacements corresponding to the unit base matrix composed of boundary forces. Therefore, matrix $\mathbf{D}$ may be treated as the dynamical flexibility matrix of the segment corresponding to a fixed value of the circular frequency $\omega$.

## 3. Analysis of roots $\chi_i(p)$

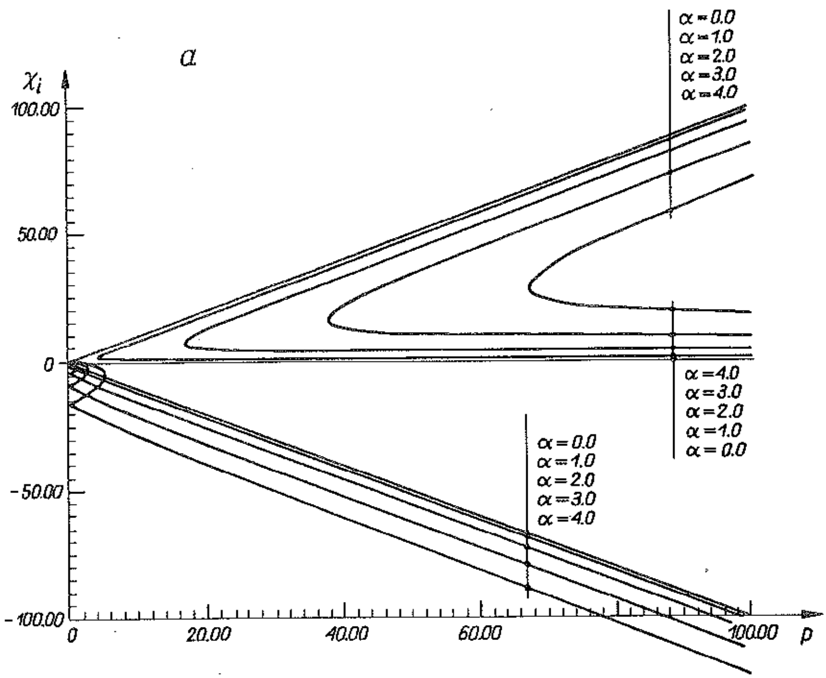


[Fig. 2a]

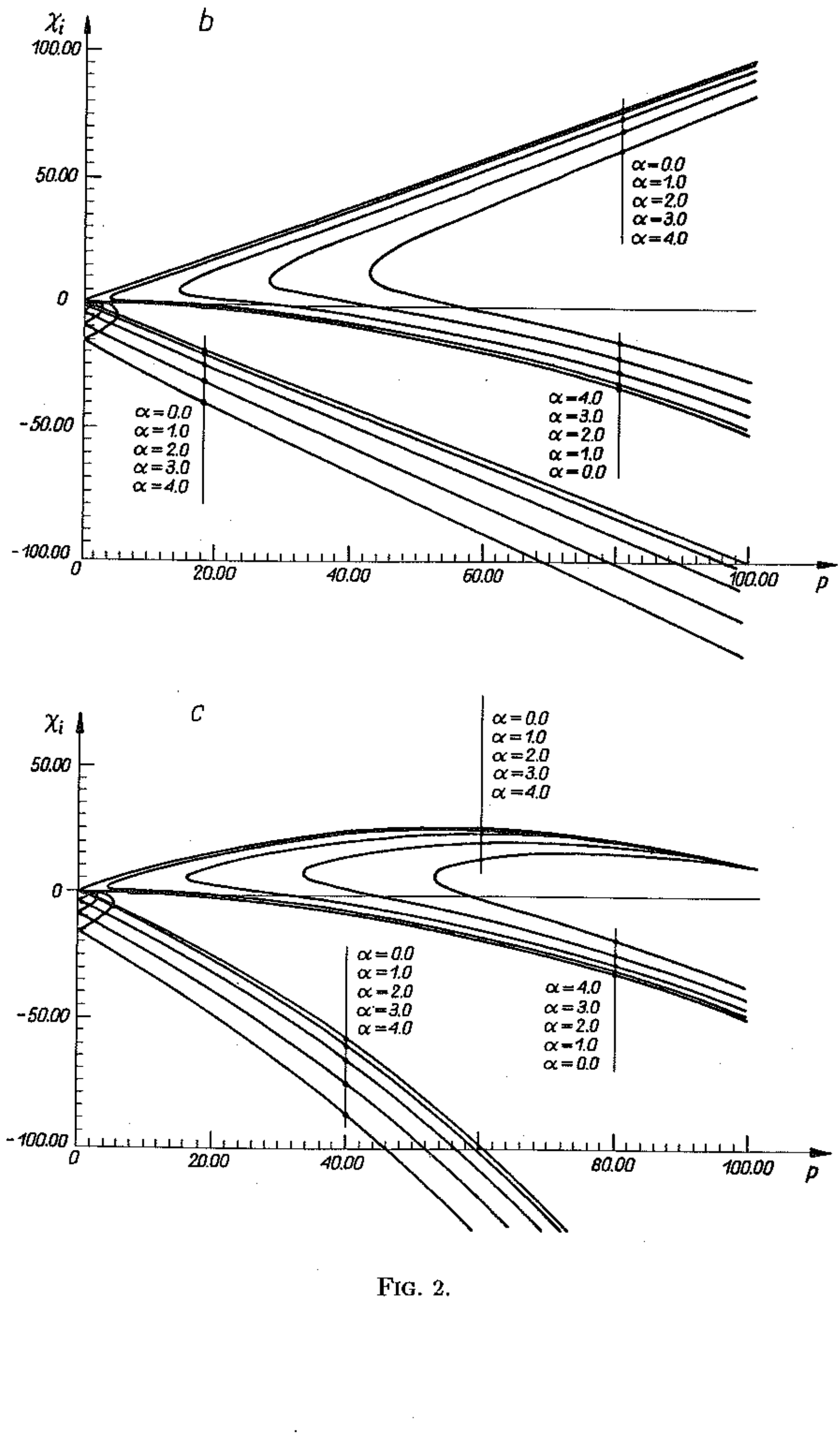
b
$\chi_i$
100.00
50.00
0
-50.00
-100.00
0
20.00
40.00
60.00
100.00
p
α = 0.0
α = 1.0
α = 2.0
α = 3.0
α = 4.0
α = 4.0
α = 3.0
α = 2.0
α = 1.0
α = 0.0
α = 0.0
α = 1.0
α = 2.0
α = 3.0
α = 4.0
c
$\chi_i$
50.00
0
-50.00
-100.00
0
20.00
40.00
80.00
100.00
p
α = 0.0
α = 1.0
α = 2.0
α = 3.0
α = 4.0
α = 0.0
α = 1.0
α = 2.0
α = 3.0
α = 4.0
α = 4.0
α = 3.0
α = 2.0
α = 1.0
α = 0.0

FIG. 2.

Construction of the universal generator of base solutions required a detailed analysis of the functions $\chi_i(p)$ $i = 1,2,3$. Dependences $\chi_i$ on $p$ are plotted in Figs. 2a,b,c for three models (BEi, BEe and RT) as the corresponding families of curves in relation to parameter $\alpha$. These plots reveal that Eq.(2.5) has not always three real roots. For parameter values belonging to the interval $[p_l(\alpha), p_u(\alpha)]$ there exists one real root only and a pair of complex conjugate ones.

In the case of a straight RT-bar ($\alpha = 0$), the coefficients (2.6) are defined by simpler formulae

$$K_2 = (r\nu_1 + \nu_2 + \nu_3)p^2, \qquad K_1 = -\nu_1 p^2 + [\nu_2\nu_3 + r\nu_1(\nu_2 + \nu_3)]p^2,$$
$$K_0 = \nu_1\nu_2 p^4(r\nu_3 p^2 - 1)$$

and Eq.(2.5) takes the form

$$(\chi + \nu_2 p^2)[\chi^2 + (r\nu_2 + \nu_3)p^2\chi + \nu_1 p^2(r\nu_3 p^2 - 1)] = 0$$

enabling an independent calculation of the eigenfrequencies corresponding to extensional or bending vibration of the bar. In the case of a BEe-model there is $r = \nu_3 = 0$, and we obtain the simplest equation

$$(\chi + \nu_2 p^2)(\chi^2 - p^2) = 0$$

represented in Fig. 2a by three lines $\chi_1 = -p$, $\chi_2 = -\nu_2 p^2$, $\chi_3 = p$.

## 4. Base generation algorithm

In order to generate all elements of the base (2.9) we have to solve a complex eigenvalue problem (2.4). In such a case the solution may be obtained efficiently by means of a slightly generalized author's method [1].

For calculation of the eigenvalues we shall use Eq.(2.5). There are three possible cases (Fig.2): 1) when $\chi_k > 0$, we have $\lambda_{2k-1} = \rho_k$, $\lambda_{2k} = -\rho_k$; 2) when $\chi_k < 0$, we have $\lambda_{2k-1} = i\sigma_k$, $\lambda_{2k} = -i\sigma_k$; 3) when $\chi_k$ is a complex root then there exists also the corresponding complex conjugate root $\bar{\chi}_k$ and we have $\lambda_{2k-1} = \rho_k + i\sigma_k$, $\lambda_{2k} = \rho_k - i\sigma_k$, $\lambda_{2k+1} = -\rho_k - i\sigma_k$, $\lambda_{2k+2} = -\rho_k + i\sigma_k$.

Calculation of the eigenvector $\mathbf{a}_k$ corresponding to the eigenvalue $\lambda_k$ will be done by denoting for simplicity $\lambda_k \equiv \lambda$ and $\mathbf{a}_k \equiv \mathbf{a}$. The calculations are simplified by introducing the transformation [1]

$$\text{(4.1)} \qquad \mathbf{X}(\xi) = \mathbf{P}[U(\xi), N(\xi), M(\xi), W(\xi), \Phi(\xi), Q(\xi)]^T, \qquad \mathbf{a} = \mathbf{P}\mathbf{b},$$

in order to change Eq.(2.4) to the form

$$[\mathbf{L}^*(\omega) - \lambda \mathbf{I}]\mathbf{b} = \mathbf{0} \tag{4.2}$$

more convenient for the analysis. In Eq.(4.2) we have denoted

$$\mathbf{L}^*(\omega) = \mathbf{P}^T\mathbf{L}(\omega)\mathbf{P} = \begin{bmatrix} 0 & L_1^*(\omega) \\ L_2^*(\omega) & 0 \end{bmatrix}, \tag{4.3}$$

$$\mathbf{L}_1^*(\omega) = \begin{bmatrix} -\alpha & 1 & -\nu_3 \\ p^2 & 0 & \alpha \\ 0 & rp^2 & -1 \end{bmatrix}, \quad \mathbf{L}_2^*(\omega) = \begin{bmatrix} \alpha & -\nu_2 & 0 \\ 0 & 0 & -\nu_1 \\ p^2 & -\alpha & 0 \end{bmatrix}. \tag{4.4}$$

Eq.(4.2) may be rewritten in a more convenient form

$$-\lambda \mathbf{b}_1 + \mathbf{L}_1^*(\omega)\mathbf{b}_2 = \mathbf{0}, \qquad \mathbf{L}_2^*(\omega)\mathbf{b}_1 - \lambda \mathbf{b}_2 = \mathbf{0}, \qquad (\mathbf{b}_1^T, \mathbf{b}_2^T) = \mathbf{b}^T \tag{4.5}$$

enabling proper elimination of the unknowns and yelding two independent equations

$$\mathbf{L}_1(\omega)\mathbf{b}_1 = \mathbf{0}, \qquad \mathbf{L}_2(\omega)\mathbf{b}_2 = \mathbf{0}. \tag{4.6}$$

In Eq.(4.6) we have denoted

$$\mathbf{L}_1 = \mathbf{L}_1^*\mathbf{L}_2^* - \lambda^2\mathbf{I} = \begin{bmatrix} -\kappa_3 & \alpha(\nu_2+\nu_3) & -\nu_1 \\ 2\alpha p^2 & -\kappa_2 & 0 \\ -p^2 & \alpha & -\kappa_1 \end{bmatrix}, \tag{4.7}$$

$$\mathbf{L}_2 = \mathbf{L}_2^*\mathbf{L}_1^* - \lambda^2\mathbf{I} = \begin{bmatrix} -\kappa_2 & \alpha & -\alpha(\nu_2+\nu_3) \\ 0 & -\kappa_1 & \nu_1 \\ -2\alpha p^2 & p^2 & -\kappa_3 \end{bmatrix}, \tag{4.8}$$

$$\kappa_1 = \lambda^2 + r\nu_1 p^2, \quad \kappa_2 = \lambda^2 + \alpha^2 + \nu_2 p^2, \quad \kappa_3 = \lambda^2 + \alpha^2 + \nu_3 p^2. \tag{4.9}$$

It is easy to verify that in case when $\lambda$ is an eigenvalue of Eq.(4.2) it has a general nontrivial solution defined by the formula

$$\mathbf{b} = \begin{bmatrix} \kappa_1\kappa_2 \\ 2\alpha\kappa_1 p^2 \\ (2\alpha^2 - \kappa_2)p^2 \\ \alpha\kappa_1(\kappa_2 - 2\nu_2 p^2)/\lambda \\ \nu_1(\kappa_2 - 2\alpha^2)p^2/\lambda \\ \kappa_1(\kappa_2 - 2\alpha^2)p^2/\lambda \end{bmatrix}. \tag{4.10}$$

Table 1.

| | Complex roots | | Imaginary roots | Real roots | |
|---|---|---|---|---|---|
| $\lambda$ | $\rho+i\sigma$ | $-\rho-i\sigma$ | $i\sigma$ | $\rho$ | $-\rho$ |
| $\bar{\lambda}$ | $\rho-i\sigma$ | $-\rho+i\sigma$ | $-i\sigma$ | | |
| $\mathbf{b}$ | $\mathbf{b}'+i\mathbf{b}''$ | $\mathbf{b}'_*+i\mathbf{b}''_*$ | $\mathbf{B}'_1+i\mathbf{B}''_2$ | $\mathbf{b}'$ | $\mathbf{b}'_*$ |
| $\bar{\mathbf{b}}$ | $\mathbf{b}'-i\mathbf{b}''$ | $\mathbf{b}'_*-i\mathbf{b}''_*$ | $\mathbf{B}'_1-i\mathbf{B}''_2$ | | |

$$\mathbf{b}'=\begin{bmatrix}\mathbf{b}'_1\\ \mathbf{b}'_2\end{bmatrix},\quad \mathbf{b}'_*=\begin{bmatrix}\mathbf{b}'_1\\ -\mathbf{b}'_2\end{bmatrix},\quad \mathbf{b}''=\begin{bmatrix}\mathbf{b}''_1\\ \mathbf{b}''_2\end{bmatrix},\quad \mathbf{b}''_*=\begin{bmatrix}\mathbf{b}''_1\\ -\mathbf{b}''_2\end{bmatrix}$$

$$\mathbf{b}=\mathbf{b}'+i\mathbf{b}'',\quad \mathbf{B}'_1=\frac{1}{2}(\mathbf{b}'+\mathbf{b}'_*),\quad \mathbf{B}''_2=\frac{1}{2}(\mathbf{b}''-\mathbf{b}''_*)$$

Owing to the fact that every pair $(\lambda,\bar{\lambda})$ of complex conjugate eigenvalues of Eq.(4.2) is related to the corresponding pair $(\mathbf{b},\bar{\mathbf{b}})$ of its eigenvectors (Table 1), we may always transform a pair of complex conjugate solutions of Eq.(2.1)

$$(\mathbf{X}(\xi),\bar{\mathbf{X}}(\xi))=\mathbf{P}\,(\mathbf{Y}(\xi),\bar{\mathbf{Y}}(\xi))=\mathbf{P}(\mathbf{b}e^{\lambda\xi},\bar{\mathbf{b}}e^{\bar{\lambda}\xi}),$$

into the equivalent pair of their real solutions $(\mathbf{F}(\xi),\mathbf{G}(\xi))$.
This complex transformation has the form

$$(\mathbf{F}(\xi),\mathbf{G}(\xi))=\frac{1}{2}(\mathbf{Y}(\xi),\bar{\mathbf{Y}}(\xi))\begin{bmatrix}1 & -i\\ 1 & i\end{bmatrix}$$

$$=\left\{e^{\rho\xi}[\mathrm{Re}(\mathbf{b})\cos(\sigma\xi)-\mathrm{Im}(\mathbf{b})\sin(\sigma\xi)],\ \ e^{\rho\xi}[\mathrm{Im}(\mathbf{b})\cos(\sigma\xi)+\mathrm{Re}(\mathbf{b})\sin(\sigma\xi)]\right\},$$

with $\rho=0$ in the purely imaginary case.

Thus, having calculated all the six eigenvalues $\lambda_k$ from Eq.(2.5) at an arbitrarily assumed, fixed value of parameter $p$ and the six corresponding eigenvectors $\mathbf{b}_k$ from formula (4.10), we can always transform the complex solution basis created for Eq(2.1) into the equivalent real one.

## 5. Results of computation

The range of computation and its results discussed below were limited to the eigenfrequencies of simply supported arches only. The values of physical parameters $\nu_1,\nu_2,\nu_3$ were assumed (see [1]) to be: $\nu_1=1$ for all types of models, $r = \nu_2 = \nu_3 = 0$ for BEi, $\nu_2 = 0.0049$, $r = \nu_3 = 0$ for BEe and $r = \nu_2 = 0.0048$, $\nu_3 = 0.01536$ for RT.

In order to simplify the comparative analysis we have introduced a new frequency parameter, the so-called comparative frequency $f$. This parameter is related to $p$ by the formula

$$f = 4p/\pi^2 .$$

Hence the circular frequency is

$$\omega = f(\pi^2/(2L)^2)\sqrt{EI/(m\bar{A})} ,$$

and the eigenspectrum for BEi-model when $\alpha = 0$ is represented by a convenient sequence of the squares of successive natural numbers: $1, 4, 9, 16, \ldots$ .

The curves $f_i$, $i = 1, 2, 3, \ldots$, representing functional dependences of successive eigenfrequencies on the value of angle $\alpha$ are shown in Figs. 3a, 3b and 3c, respectively, for models BEi, BEe, RT and values $\alpha \leq 3.0$, $f_i \leq 20.0$. The calculated frequencies are listed and compared in Table 2 for certain values of parameter $\alpha$.

Table 3 contains a comparison of results obtained by means of the new algorithm with those calculated from Goldenblat's formulae [11]. The most compatible results (error less than 0.05%) in the whole range of values $\alpha$ we observe for the eigenfrequencies corresponding to antisymmetrical, one-node vibration modes. We may recognize as quite satisfactory too the results

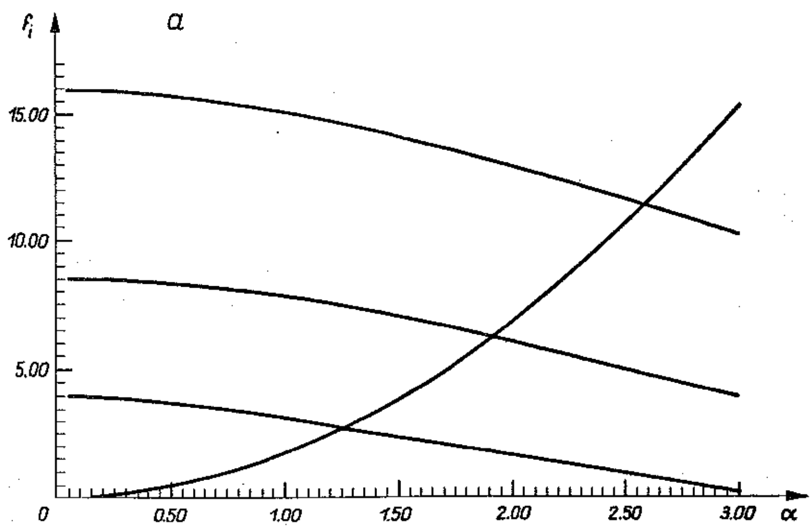


[Fig. 3a]

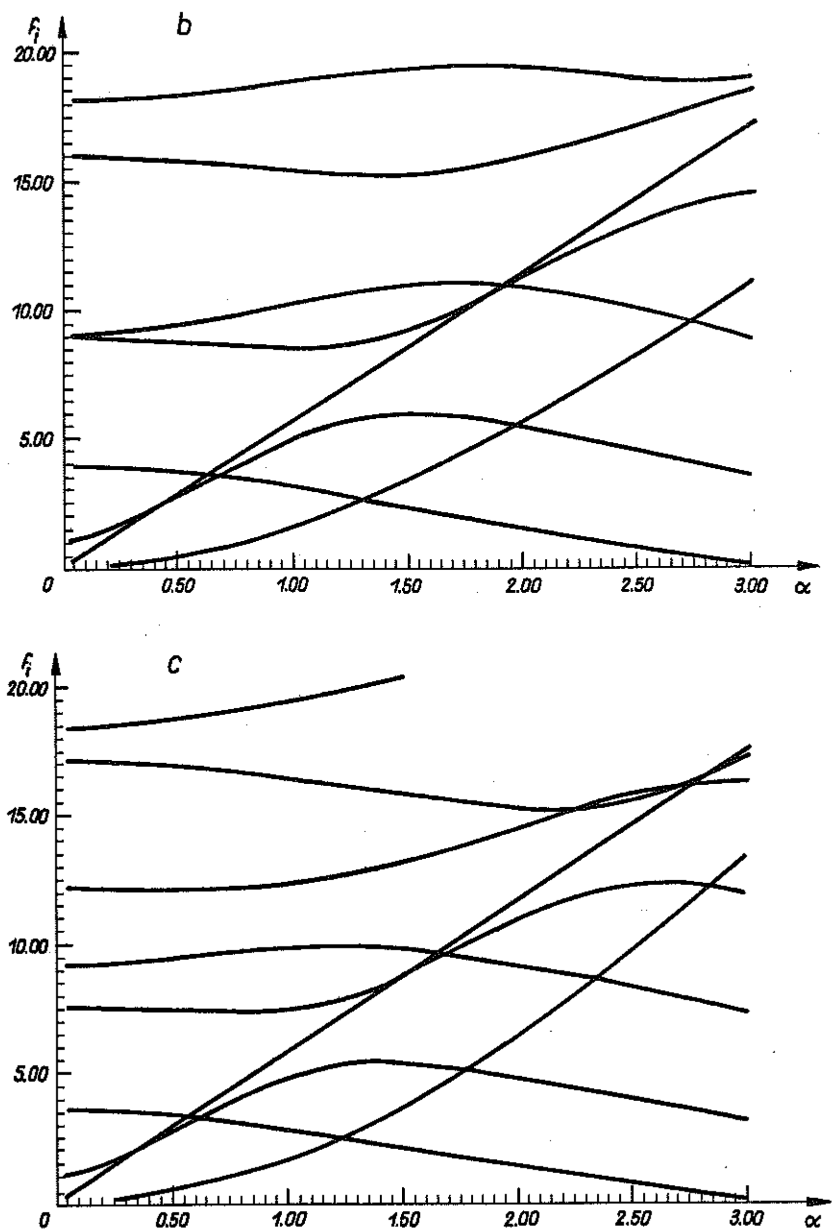
b
$f_i$
20.00
15.00
10.00
5.00
0
0.50
1.00
1.50
2.00
2.50
3.00
α
c
$f_i$
20.00
15.00
10.00
5.00
0
0.50
1.00
1.50
2.00
2.50
3.00
α

FIG. 3.

Table 2.

| $\alpha =$ | 0.5 | 1.0 | 1.5 | 2.0 | 2.5 | 3.0 |
|---|---|---|---|---|---|---|
| BEn | 0.425508 | 1.70203 | 2.37872 | 1.59727 | 0.861202 | 0.182342 |
| | 3.75841 | 3.14740 | 3.82957 | 6.08024 | 5.00909 | 3.91005 |
| | 8.35962 | 7.84036 | 7.05177 | 6.80813 | 10.6377 | 10.2070 |
| | 15.7545 | 15.0903 | 14.1317 | 12.9641 | 11.6412 | 15.3183 |
| | | | | | | 18.8603 |
| BEr | 0.420201 | 1.62219 | 2.29825 | 1.54501 | 0.836503 | 0.177893 |
| | 2.76010 | 3.06104 | 3.46093 | 5.56153 | 4.65492 | 3.66762 |
| | 2.89489 | 4.99762 | 6.05388 | 5.76678 | 8.39099 | 9.05232 |
| | 3.71582 | 5.78978 | 8.68467 | 11.0095 | 10.1985 | 11.2215 |
| | 8.83922 | 8.57231 | 9.27580 | 11.3197 | 13.4355 | 14.6274 |
| | 9.47983 | 10.3482 | 11.0795 | 11.5796 | 14.4745 | 17.3693 |
| | 15.8409 | 15.4842 | 15.3432 | 15.9883 | 17.2829 | 18.6694 |
| | 18.4049 | 18.9354 | 19.4450 | 19.4690 | 19.0456 | 19.1696 |
| RT | 0.424174 | 1.68048 | 2.13674 | 1.43746 | 0.776960 | 0.164632 |
| | 2.75755 | 2.83488 | 3.71879 | 4.87384 | 4.06789 | 3.21164 |
| | 2.92489 | 4.88850 | 5.44558 | 6.45189 | 8.37353 | 7.38263 |
| | 3.41750 | 5.84978 | 8.77467 | 9.23487 | 9.75353 | 12.0215 |
| | 7.45238 | 7.44863 | 8.81043 | 10.9684 | 12.3281 | 13.4624 |
| | 9.47155 | 9.93134 | 9.84479 | 11.6996 | 14.6245 | 16.3058 |
| | 12.1540 | 12.3463 | 13.2170 | 14.5485 | 15.5842 | 17.3355 |
| | 16.9585 | 16.4536 | 15.8524 | 15.3145 | 15.7943 | 17.5493 |
| | 18.7159 | 19.4608 | | | | |

obtained for $\alpha \geq 1.0$ in the case of symmetrical nodeless vibration modes. For values $\alpha < 1.0$ there is a rapid increase of error combined even with the change of sign. This is most probably caused by a qualitative change in the dynamical behaviour of vibrating segment disregarded by the Goldenblat's formulae. Frequencies of two- or three-node vibration modes reveal several percent errors. For antisymmetric three-node vibration, however, when $\alpha \leq 1.5$, the results may be recognized as quite satisfactory again.

On the basis of Fig.3 we may state that the models considered and, especially the RT-model, reveal quite complex dynamical properties as functions of angle $\alpha$, represented by their eigenspectra. This complexity causes substantial problems in complete verification of the numerical results, especially for RT-model, because no adequate references in the corresponding literature can be found thus far.

Variable structure of eigenspectra (appearance of multiple or very close eigenfrequencies) observed in the models under consideration makes the application of approximate methods (Ritz, FEM) unreliable and demands special care.

Table 3.

| Mode | I symmetrical (nodeless) | | | I antisymmetrical (one-node) | | |
|---|---|---|---|---|---|---|
| $\alpha$ | BEr | GOL | Δ% | BEn | GOL | Δ% |
| 0.0 | 0.0000 | 1.0000 | | 4.0000 | 4.0000 | 0.000 |
| 0.5 | 3.7158 | 3.0627 | −17.6 | 3.7584 | 3.7585 | 0.003 |
| 1.0 | 5.7898 | 5.8755 | 1.48 | 3.1474 | 3.1480 | 0.019 |
| 1.5 | 8.6847 | 8.7421 | 0.66 | 2.3787 | 2.3798 | 0.046 |
| 2.0 | 11.580 | 11.623 | 0.37 | 1.5973 | 1.5981 | 0.051 |
| 2.5 | 14.474 | 14.509 | 0.24 | 0.86120 | 0.86147 | 0.031 |
| 3.0 | 17.369 | 17.398 | 0.17 | 0.18234 | 0.18235 | 0.005 |

| Mode | II symmetrical (two-node) | | | II antisymmetrical (three-node) | | |
|---|---|---|---|---|---|---|
| $\alpha$ | BEr | GOL | Δ% | BEn | GOL | Δ% |
| 0.0 | 9.0000 | 9.0000 | 0.00 | 16.000 | 16.000 | 0.00 |
| 0.5 | 8.3596 | 8.8251 | 5.57 | 15.755 | 15.750 | −0.03 |
| 1.0 | 7.8404 | 8.3207 | 6.13 | 15.090 | 15.034 | −0.37 |
| 1.5 | 7.0518 | 7.5401 | 6.92 | 14.132 | 13.943 | −1.34 |
| 2.0 | 6.0802 | 6.5533 | 7.78 | 12.964 | 12.592 | −2.87 |
| 2.5 | 5.0091 | 5.4299 | 8.40 | 11.641 | 11.089 | −4.74 |
| 3.0 | 3.9100 | 4.2281 | 8.14 | 10.207 | 9.5190 | −6.74 |

Note: GOL – results from [11]

## 6. Final remarks

The concept of the new universal algorithm for base generation discussed in the present paper was verified in computational practice and proved to be numerically very efficient. This efficiency was used effectively in the eigenproblem analysis for simply supported circular arches (segments) in order to reveal complex functional dependences of their eigenspectra on the subtending angle $2\alpha$. The plots of these functions reveal true complexity of dynamical eigenproblems of circular arches and enable us to create a foundation for verification of the results obtained by approximate methods.

Calculation of the eigenspectra of arches with boundary conditions other than simply supported and application of the base generator in computing their stiffness and flexibility matrices require separate description and are out of the scope of the present paper.

## References


1. B.Olszowski, *Free in-plane vibrations of unsupported circular rings. Part I. Natural frequencies*, Rozpr. Inż., **37**, 3, 547-563, 1989; *Part II. Natural modes*, Rozpr. Inż., **38**, 3-4, 529-547, 1990; *Part III. Free single-frequency vibrations*, Rozpr. Inż., **38**, 3-4, 549-565, 1990.
2. V.Koloušek, *Dynamics in engineering structures*, Butterworths, London 1973.
3. B.Åkesson, H.Tägnfors and O.Johannesson, *Beams and frames in bending vibration* [in Swedish], Almqvuist and Wiksell, Stockholm 1972.
4. B.Åkesson and H.Tägnfors, PFVIBAT – *A computer program for plane frame vibration analysis*, Publ. No. 25, Chalmers Univ. of Technol., Div. of Solid Mech., Gothenburg 1974.
5. W.H.Wittrick and F.W.Williams, *A general algorithm for computing natural frequencies of elastic structures*, Q.J. Mech. Appl. Math., **24**, 263-284, 1971.
6. R.Lunden and B.Åkesson, *Damped second-order Rayleigh-Timoshenko beam vibration in space – an exact complex dynamic member stiffness matrix*, Int. J. Num. Meth. Engng., **19**, 3, 431-449, 1983.
7. P.O.Friberg, *Coupled vibrations of beams – an exact dynamic element stiffness matrix*, Int. J. Num. Meth. Engng., **19**, 479-493, 1983.
8. P.O.Friberg, *Beam element matrices derived from Vlasov's theory of open thin-walled elastic beams*, Div. of Solid Mech., Chalmers Univ. of Technol., Gothenburg 1984.
9. M.S.Issa, T.M.Wang and B.T.Hsiao, *Extensional vibrations of continuous circular curved beams with rotary inertia and shear deformation, I. Free vibration*, J. Sound and Vibr., **114**, 2, 297-308, 1987.
10. T.M.Wang and M.S.Issa, *Extensional vibrations of continuous circular curved beams with rotary inertia and shear deformation*, II. *Forced vibration*, J. Sound and Vibr., **114**, 2, 309-323, 1987.
11. **И.И.Гольденблат, А.М.Сизов, Справочник по расчету строительных конструкций на устойчивость и колебания, Гос. Изд. Литер. по Строит. и Арх., Москва 1952.**


KRAKÓW UNIVERSITY OF TECHNOLOGY.

*Received August 14, 1991.*